Proteomic survey of the DNA damage response in *Caulobacter crescentus* reveals evidence of post-transcriptional control

Running Title: Survey of post-transcription control upon DNA damage

Tommy F. Tashjian[#], Rilee D. Zeinert[*], Stephen J. Eyles, Peter Chien[#]

Department of Biochemistry and Molecular Biology, University of Massachusetts Amherst, Amherst, MA, USA

*Current address: Cell Biology and Metabolism Program, Eunice Kennedy Shriver National Institute of Child Health and Human Development, Bethesda, MD 20892-5430, USA

#co-corresponding authors:

Tommy Tashjian, Department of Biochemistry and Molecular Biology, University of Massachusetts Amherst, Life Science Laboratories Room N325, 240 Thatcher Rd, Amherst MA 01003-9364, (413)545-2310, ttashjian@umass.edu

Peter Chien, Department of Biochemistry and Molecular Biology, University of Massachusetts Amherst, Life Science Laboratories Room N325, 240 Thatcher Rd, Amherst MA 01003-9364, (413)545-2310, pchien@umass.edu;

ABSTRACT

The bacterial DNA damage response is a critical, coordinated response to DNA replication stress. The canonical bacterial DNA damage response, first characterized in *Escherichia coli*, is controlled by the global transcriptional regulator LexA and the recombinase RecA. While genome-wide studies have described how the DNA damage response is regulated at a transcriptional level, relatively little is known about post-transcriptional regulation of this response. Here, we perform a proteome-wide survey of the DNA damage response in *Caulobacter crescentus*. We find that not all changes in protein abundance during the response to DNA damage are predicted by changes in transcription. We validate one of these post-transcriptionally regulated candidates to show its importance to survival of DNA damage. To investigate post-translational control of the DNA damage response, we perform a similar survey in cells lacking the Lon protease. This reveals that induction of the DNA damage response at the protein level is dampened in these strains, consistent with their reduced tolerance to DNA damage. Finally, proteome-wide stability measurements following damage nominate candidate Lon substrates that suggest post-translational regulation of the DNA damage response.

IMPORTANCE

The DNA damage response helps bacteria to respond to and potentially survive DNA damage. The mutagenesis that is induced as part of this response plays a role in bacterial evolution and is essential to the development and spread of antibiotic resistance. Understanding how bacteria coordinate their response to DNA damage could help us to combat this growing threat to human health. While the transcriptional regulation of the

40 bacterial DNA damage response has been characterized, this study is the first to our
41 knowledge to compare changes in RNA and protein levels to identify potential targets of
42 post-transcriptional regulation in response to DNA damage.

43 **INTRODUCTION**

44 The bacterial DNA damage response is tightly linked to the mutagenesis that drives
45 bacterial evolution, antibiotic resistance development, and the horizontal gene transfer
46 that spreads resistance from cell to cell. The canonical DNA damage response was first
47 characterized in *Escherichia coli*. During DNA damage ssDNA accumulates in the cell
48 and is bound by the cell's main recombinase RecA to form a nucleoprotein filament that
49 induces the autocleavage of the global transcriptional repressor LexA (1, 2). Cleavage of
50 the repressor LexA promotes transcription of more than 40 genes related to DNA damage
51 tolerance and repair (3, 4).

52 In addition to LexA-mediated transcriptional regulation, the DNA damage response is also
53 controlled by sRNA, protein-protein interactions, and proteolysis. For example, in *E. coli*,
54 the toxin TisB is regulated by LexA and by the antitoxin sRNA IstR1 (5, 6). Similarly,
55 during the *Caulobacter crescentus* DNA damage response expression of the TonB
56 receptor ChvT is inhibited by the sRNA ChvR (7). Alternatively, the activity of several DNA
57 damage proteins are regulated by protein-protein interactions (e.g. DinB (8, 9), MutS and
58 MutL reviewed in (10)). Finally, proteolysis plays a key role in the induction (through
59 degradation of remnants of cleaved LexA (11)) and shut down of the DNA damage
60 response (by degrading key proteins at the end of the response, e.g. UmuD' (12) and

61 UvrA (13)). Given these examples of post-transcriptional regulation for DNA damage, we
62 reasoned that a proteomics survey of this same stress would be valuable.

63 Compared to *E. coli*, we have limited knowledge of the DNA damage response in
64 *Caulobacter*. This alphaproteobacteria also contains a coordinated DNA damage
65 response that is controlled by the global transcriptional repressor LexA (14–16). A second
66 DNA damage-controlled transcriptional repressor DriD that, like LexA, responds to ssDNA
67 (16, 17), is also involved in the induction of another set of DNA damage response genes
68 (16). Other than the discovery of ChvR (7) described above, little is known about the role
69 of post-transcriptional regulation in *Caulobacter's* DNA damage response.

70 In the first stage of our proteomics study, we surveyed post-transcriptional regulation of
71 the DNA damage response in *Caulobacter*. As expected, we found a high level of synergy
72 between the transcriptional regulation of the response and the changes in protein
73 abundance upon DNA damage. We were also able to identify proteins that appear to be
74 regulated post-transcriptionally during the DNA damage response and explored their
75 physiological impact. In the second stage of this study, we examined protein stability
76 upon DNA damage. As expected after translational shutoff, we detected protein level
77 decreases in several known proteolysis substrates. In addition, some of the proteins that
78 were induced upon DNA damage are also candidate proteolysis substrates.

79 Our data show that not all protein abundance changes during the DNA damage response
80 are driven by transcriptional control and identify novel *Caulobacter* DNA damage
81 response factors that are likely regulated post-transcriptionally.

82 **RESULTS**

83 **Proteomics identify upregulated DNA damage response factors**

84 To characterize protein abundance changes during the DNA damage response, we first
85 used the sentinel protein RecA to determine the timescale of an acute mitomycin C (MMC)
86 treatment in *Caulobacter* (Figure 1A). Based on this characterization, we compared whole
87 cell proteome abundances using mass spectrometry before and after MMC treatment
88 (timeline described in Figure 1A, full list of results in Table S1 and S2). The post-MMC
89 timepoint was taken at the timepoint that showed the highest RecA concentration by
90 western blot (Figure 1A). As expected, we found several DNA damage response proteins
91 to be more abundant after MMC treatment (RecA, UvrA, RuvB, ImuA, and MmcA; Figure
92 1B). To characterize our dataset further, we compared changes in protein abundance
93 observed by our proteomics approach to published changes in RNA levels upon MMC
94 treatment (15), to those genes predicted to be regulated by LexA (14), and to potential
95 fitness effects observed by transposon sequencing (Table S3).

96 Past work has explored transcriptional responses to DNA damage in Caulobacter,
97 including bioinformatic predictions of LexA binding sites (14), RNA-seq during extended
98 chronic damaging conditions (7), and microarray experiments with a variety of damaging
99 conditions (15). Based on consistency with our experimental design we used Modell, et
100 al. as a comparison (15). In this study, transcript levels were monitored using microarrays
101 over several time points after MMC treatment in rich medium (15). To identify genes that
102 are transcriptionally upregulated upon MMC treatment, we used the maximum $\log_2$(Fold
103 Change of RNA) from these timepoints for each gene and treated genes that were
104 induced more than one standard deviation above the mean as "upregulated". This
105 threshold is intentionally inclusive to capture even weakly induced genes, as we are

106 particularly interested in identifying genes that are not upregulated transcriptionally in our
107 next analysis step.

108 This strategy yielded in 615 upregulated genes of which 146 could be identified as
109 peptides in our proteomics survey. Of these, 43 show significant increase in protein
110 abundance upon DNA damage (Table S4, $\log_2$(3 hrs/0 hrs) > 0, FDR < 0.05). As
111 expected, the known DNA damage proteins mentioned above that showed increased
112 protein abundances following MMC treatment were also significantly upregulated at the
113 RNA level (Figure 1B). These findings validate that our proteomics approach and data
114 analysis methods can be used to successfully identify genes upregulated during the DNA
115 damage response. There are some limitations, as no peptides were identified for a
116 number of DNA damage response proteins predicted to be upregulated by microarray
117 ((15), e.g. SidA, DidA, DnaE2).

118 **Post-transcriptional control of DNA damage response proteins**

119 We identified 81 proteins that significantly increased in abundance upon DNA damage
120 ($\log_2$(Fold Change in Protein) > 0, FDR < 0.05) and did not show a corresponding
121 significant increase in RNA level ((15), Table S5). Some of these are known to be involved
122 in DNA replication (*dnaA*, *dnaQ*) or repair (*radA*) and one is a homolog of the DNA repair
123 helicase *dinG* (CCNA_02118). In addition, three proteins involved in response to oxidative
124 stress were found in this list (two superoxide dismutase proteins: CCNA_01650,
125 CCNA_03672, and a hyperoxide resistance protein: CCNA_00963). None of these genes
126 are predicted to be transcriptionally regulated by LexA (14) or *Caulobacter's* LexA-

127 independent DNA damage response (16) but protein abundances indicate that they are
128 upregulated upon DNA damage.

129 Two of the 81 genes (CCNA_03496: *yaaA* and CCNA_00276: hypothetical protein) are
130 of particular interest, as our Tn-seq experiments identified them as potentially important
131 for survival of MMC (Table S3). CCNA_03496 is a homolog of *E. coli*'s *yaaA* ((18), we will
132 refer to this gene as *yaaA* henceforth), which is important for regulating iron levels during
133 oxidative stress conditions (19). CCNA_00276 is a hypothetical cupin superfamily protein.
134 Based on published RB-Tnseq results, strains carrying transposon insertions in *yaaA* or
135 CCNA_00276 have a sensitivity to the DNA damaging agent cisplatin (20). For these
136 reasons, we decided to further characterize the connection between these genes and
137 MMC survival.

138 Contrary to our expectations, deletion of these genes had no effect on growth of isolated
139 cultures with MMC (Figure S2A and S2B). To focus on fitness differences, we turned to
140 a competition assay. We observed that a Δ*yaaA* strain expressing the mKate2 fluorescent
141 protein is significantly less able than the wild type mKate2-expressing strain to compete
142 in co-culture with a wild type control expressing the Venus fluorescent protein (Figure
143 2C). This competitive disadvantage becomes significantly worse in the presence of MMC
144 (Figure 2C). By contrast, the ΔCCNA_00276 (denoted as Δ276 throughout) does not
145 show a disadvantage (Figure 2C). To confirm that these results are not an artifact of the
146 fluorescent strains, we flipped the markers to test Venus-expressing deletion strains
147 against mKate2-expressing controls and saw similar results (Figure S2C). These data
148 support our hypothesis that YaaA plays a role in the DNA damage response.

149 Finally, we note that of the 146 genes that are transcriptionally upregulated upon DNA
150 damage and were identified in our proteomics, 103 showed no significant increase in
151 protein level (Table S6). Two of these proteins have known roles in DNA repair (UvrD and
152 RecN) and one is a homolog of the DNA recombination protein RmuC (CCNA_00272).
153 An increase in RNA levels without a corresponding increase in protein levels suggests
154 some level of post-transcriptional regulation.

155 **Identification of factors that are downregulated and important for MMC survival**

156 We next looked at those genes downregulated following MMC damage. We used the
157 minimum $\log_2$(Fold Change of RNA) from the Laub lab microarray timepoints for each
158 gene for the transcriptional response (15). To ensure inclusion for even weakly regulated
159 genes, a transcript that is more than one standard deviation below the mean of these
160 values was considered "downregulated". With these criteria, we identified 614 genes that
161 are downregulated upon DNA damage. Of these, 292 were identified in our proteomics
162 (Figure 3A).

163 We identified 99 proteins that became significantly less abundant upon DNA damage and
164 did not show a decrease in RNA abundance (Table S7). These are proteins that may be
165 post-transcriptionally downregulated during the DNA damage response, and include
166 known DNA replication factors DNA gyrase A, DNA gyrase B, and topoisomerase I. Our
167 Tn-seq results identified six of these genes as more likely to contain transposon insertions
168 upon MMC damage: CCNA_03681: ABC transporter ATP-binding protein, CCNA_00299:
169 PurD, CCNA_00099: FzlC, CCNA_01034: TonB-dependent outer membrane receptor,
170 and CCNA_01817: NtrX. We decided to focus on PurD and FzlC for further

171 characterization as membrane proteins may alter MMC import and NtrX might have
172 confounding effects because of its role in cell cycle regulation (21, 22).

173 The gene *purD* (CCNA_00299) encodes phosphoribosylamine-glycine ligase, which
174 catalyzes the second step of *de novo* purine biosynthesis. *Caulobacter* RB-Tnseq-based
175 fitness results suggest that transposon insertions in this gene can lead to increased
176 survival of nalidixic acid (20). While we did not observe any benefit to MMC survival in the
177 Δ*purD* strain (Figure 3B), we found that a *ΔpurD* strain of *Caulobacter* has a relative
178 stationary phase defect in rich medium not observed during MMC treatment (Figure 3B).
179 The mutant reaches a maximum density earlier than the wildtype with a final optical
180 density 14% lower than that of the wild type strain. In the presence of MMC, this difference
181 is lost, resulting in *ΔpurD* strains showing a relative fitness improvement during damage
182 compared to undamaged conditions, consistent with published Tn-seq results (20) and
183 our own results (Table S3).

184 FzlC (CCNA_00099) is a component of the *Caulobacter* cell division machinery that
185 anchors FtsZ to the membrane (23). Because of the connection between cell division and
186 DNA repair, we chose to investigate this gene further but found that deletion of *fzlC* did
187 not have any impact on MMC-sensitivity by growth curve (Figure 3C) or competition
188 experiment (Figure S3).

189 **Identification of potential Lon substrates induced by the DNA damage response**

190 To investigate the role of post-translational regulation during the DNA damage response,
191 we performed proteomics in a strain lacking the dispensable Lon protease. By performing
192 the same proteomics experiment as above in a *Δlon* strain (full dataset in Table S1 and

193 S2), we can observe how loss of Lon proteolysis affects protein induction during DNA
194 damage. Similar to the wild type strain, we monitored RecA levels through induction and
195 recovery after MMC treatment in ∆lon (Figure 4A). We find that the peak induction occurs
196 at a similar time point in the wild type (Figure 1A) and Δ*lon* strains (Figure 4A) but the
197 fold-induction of RecA in the Δ*lon* strain is less than half that in the wild type strain. We
198 reasoned that this was due to upregulation of DNA damage response genes in a Δ*lon*
199 strain even in the absence of exogenous DNA damaging agents (24). Most of the detected
200 known DNA damage-related proteins upregulated upon MMC treatment in the wild type
201 strain are also upregulated in the Δ*lon* strain (See RecA, RuvB, and MmcA in Figure 4B).
202 The exceptions here are UvrA, which is not significantly induced at the protein level in the
203 Δ*lon* strain (Figure 4B) and ImuA, which was not identified in the proteomics of the Δ*lon*
204 strain. In general, the fold change in protein abundance upon DNA damage in the Δ*lon*
205 strain was reduced compared to the wild type strain (Figure 4C).

206 To monitor post-translational control during DNA damage, we measured protein
207 abundances after a translational shutoff. Specifically, we added chloramphenicol to inhibit
208 translation at the post-MMC treatment timepoint (3 hours in Figure 1A and 5A) and
209 measured protein abundances 2 hours post-translational shutoff (timeline Figure 5A, full
210 dataset in Table S1 and S2). For proteins induced as part of the DNA damage response
211 and degraded by a protease, we expected an increase in protein abundance between the
212 pre- and post-MMC treatment samples (0 and 3 hours, Figure 5A, left) and a decrease in
213 protein abundance between the pre- and post-translational shutoff samples (3 and 5
214 hours, Figure 5A, left). In wild type cells, we see this pattern for the replication initiator
215 DnaA and IbpA, known substrates of the Lon protease ((25, 26) Figure 5A, right).

216 In total, we identified 320 proteins that significantly decreased in protein abundance upon
217 translational shutoff in the wild type strain ($\log_2$(5 hrs/3 hrs) < 0, FDR < 0.05; Table S8).
218 Twenty-one of these proteins have previously been identified as ClpP substrates by a
219 ClpP trap in *Caulobacter* (27), including NrdA, DnaX, and CtrA. In addition, other known
220 ClpXP substrates (e.g., FtsZ, UvrA, LexA) and ClpAP-dependent substrates (e.g., FtsA,
221 Lon) were identified by these criteria (all mentioned proteins are highlighted in red in
222 Figure 5B).

223 We performed the same proteomics experiment during translational shutoff in MMC-
224 treated Δ*lon* cells to identify Lon substrates induced during DNA damage. Similar to
225 induction of proteins (Figure 4C), we found that protein loss in the Δ*lon* strain was
226 dampened compared the wild type strain (Figure S4). As expected from known Lon
227 substrates DnaA (25) and small heat shock protein IbpA (shown in *E. coli* (26)) are not
228 rapidly degraded upon translational shutoff in the *Δlon* strain (Figure 5C, Table S8)
229 compared to the wild type strain (Figure 5B, Table S8). Additionally, the decrease in
230 protein abundance upon shutoff is largely unchanged for ClpXP and ClpAP substrates
231 (see examples for FtsZ, FtsA, and DnaX in Figure S5).

232 To identify potential Lon substrates in this list, we compared the change in protein
233 abundance after translational shutoff for each protein in the wild type and Δ*lon* strains.
234 The 10% of proteins with the greatest difference in $\log_2$(5 hrs/3 hrs) between the two
235 strains were considered potential Lon substrates (29 candidates; Table S8). Two of these
236 proteins are the known Lon substrates DnaA (25) and a small heat shock protein IbpA
237 (26). UvrD, a DNA damage repair helicase, was also identified here.

238 Based on our results, we conclude that not all changes at the protein abundance during
239 the DNA damage response can be explained by changes in transcript level. This shutoff
240 stage of our proteomics experiments allows us to nominate candidates for post-
241 translational control through degradation.

242 **DISCUSSION**

243 Survey of protein abundance changes upon DNA damage

244 The transcriptional regulation of the DNA damage response by the RecA/LexA system
245 and the effect of DNA damage treatment on the transcriptome has been studied in the
246 canonical *E. coli* response (3, 4) and in *Caulobacter* (14, 15). Past work in gamma-
247 irradiated *E. coli* showed a correlation between proteome upregulation and transcriptional
248 changes (28). However, our work is the first to our knowledge to compare proteomic and
249 transcriptomic changes with the intent to identify targets of post-transcriptional regulation.
250 While we find that protein abundance changes upon DNA damage largely correspond to
251 changes in transcript levels, not all protein changes during *Caulobacter's* DNA damage
252 response can be explained by transcriptional effects. Because these differences could be
253 explained by a regulation at the post-transcriptional or post-translational level, we
254 augmented our survey with translational shutoff experiments to identify factors that are
255 potentially regulated by proteolysis during the DNA damage response.

256 Our observations in the Δ*lon* strain are consistent with its reduced tolerance of DNA
257 damage compared to wild type (28). While a similar set of proteins is upregulated upon
258 DNA damage in the Δ*lon* and the wild type strains, fold-inductions of proteins during the
259 DNA damage response were generally lower in the Δ*lon* strain (Figure 4). We propose

260 this is due to the fact that many DNA damage genes are already upregulated in the Δ*lon*
261 strain even in the absence of exogenous DNA damage treatment (24). These data may
262 also explain the previous observation that the Δ*lon* strain has an elevated sensitivity to
263 DNA damage (29).

264 Possible post-transcriptional regulation of known DNA damage genes

265 We were able to identify known DNA damage proteins that appear to be post-
266 transcriptionally regulated in our conditions. Some examples are discussed here.

267 In *E. coli* UvrA is known to be degraded in a DNA damage-controlled manner by ClpXP
268 (13). In *Caulobacter*, we find an increase in protein levels following DNA damage that is
269 likely due to increased transcription (Table S4, (15)). Consistent with a role for ClpXP in
270 proteolysis, we observe a Lon-independent decrease in protein abundance (Table S8)
271 upon translational shutoff. These data indicate that the proteolytic control of UvrA
272 observed in *E. coli* is likely conserved in *Caulobacter*.

273 After LexA autocleavage is induced by the RecA nucleoprotein filament, both halves of
274 LexA are proteolyzed by ClpXP in *E. coli* (11). Proteolysis of the DNA-binding N-terminus
275 of LexA is critical for DNA damage survival, likely because it prevents any residual
276 repression that may be caused by this fragment (11). Our proteomics dataset only
277 identified peptides that mapped to the N-terminus of LexA (Figure S6), which is highly
278 conserved between *E. coli* and *Caulobacter*. Upon translational shutoff we find that the
279 LexA N-terminus decreases in protein abundance upon translational shutoff in a Lon-
280 independent manner. This suggests that the proteolysis of the N-terminal LexA fragment
281 observed in *E. coli* is conserved in *Caulobacter*.

282 *E. coli radA* plays a role in recombination and survival to DNA damage (30). In the
283 hyperthermophilic archaeon *Pyrococcus horikoshii* RadA levels has been shown to be
284 controlled by protein splicing in the (31), supporting a post-translational control
285 mechanism for this protein. *Caulobacter radA* is part of an eight-gene operon with genes
286 for integral membrane proteins and amino acid metabolism (32), lacking a predicted
287 LexA-binding site (14). While transcript levels for genes in *Caulobacter radA*'s operon
288 remain constant upon DNA damage (15), RadA protein levels increase significantly upon
289 DNA damage (Table S5). We were able to detect two other proteins encoded upstream
290 of *radA* in this operon in our proteomics (CCNA_01728 and CCNA_01730) and they were
291 not upregulated at the protein level (Table S2). These observations suggest that post-
292 transcriptional regulation may play a role in the selective expression of the *Caulobacter*
293 RadA protein.

294 Finally, while DNA repair gene *uvrD* is upregulated at the transcript level (15, 16), we do
295 not see a significant increase in UvrD protein abundance upon DNA damage (Table S6).
296 Our observation that UvrD protein abundance significantly decreases after translational
297 shutoff suggests that proteolysis may play a role in its regulation. UvrD is stable upon
298 translational shutoff in the Δ*lon* strain, supporting a role for Lon in this process, either
299 through direct proteolysis of UvrD or of a second factor that regulates UvrD protein levels.

300 <u>Additional proteins regulated independent of transcription following DNA damage</u>

301 Through our studies, we discovered post-transcriptionally regulated factors that were not
302 previously known to play a role in the *Caulobacter* DNA damage response.

303 *Caulobacter* YaaA is upregulated at the protein level upon DNA damage with no
304 corresponding increase in transcript levels (15). In *E.coli, yaaA* is transcriptionally
305 regulated by OxyR, is expressed in response to oxidative stress (19, 33) and protects
306 cells from damage from the Fenton reaction by controlling intracellular levels of
307 unincorporated iron (19). In *Caulobacter*, *yaaA* does not appear to be regulated by OxyR
308 (34), but published RB-Tnseq experiments indicates that transposon insertions in *yaaA*
309 cause a sensitivity to cisplatin (20). In *E. coli* cisplatin treatment causes an increase in
310 iron uptake through downregulation of Fur (35) and *Δfur ΔyaaA* strains show a
311 synthetically lethal effect (19). These published works and our observation that Δ*yaaA*
312 *Caulobacter* has a competitive disadvantage against the wild type strain in MMC suggest
313 that *Caulobacter yaaA* could play a similar role (Figure 2C).

314 We also find evidence for post-transcriptional downregulation of proteins such as the
315 phosphoribosylamine-glycine ligase PurD, whose protein levels decrease upon DNA
316 damage without a corresponding decrease in RNA levels (Table S7). PurD is the second
317 enzyme in the bacterial purine biosynthesis pathway. In *Bacillus anthracis*, *purD* and
318 some other purine biosynthesis genes are controlled by riboswitches that deactivate
319 translation when levels of guanosine are high (36). Based on this and our proteomic
320 results, we propose that *purD* is also controlled by post-transcriptional regulation in
321 *Caulobacter*, though it is not clear why downregulation of purine biosynthesis would be
322 beneficial during the DNA damage response. One possibility is that this is a side-effect of
323 MMC crosslinking, possibly by disrupting function of a cis- or trans-acting element
324 regulating translation of the *purD* mRNA. Another possibility is that guanosine derivatives

325 (such as ppGpp (37)), which are upregulated during DNA damage, may be affecting
326 translation of this gene.

327 Concluding thoughts

328 In our proteomics analysis, we identified and quantified protein abundances for about
329 30% of the *Caulobacter* proteome. While some of the missing proteins are likely not
330 expressed during the growth conditions of our assays, some key DNA damage response
331 proteins are missing from our dataset. Some of these are known to be membrane-
332 associated (e.g. SidA (15) and DidA (16)), which may reduce our detection, and others
333 are likely have relatively low abundance, even during DNA damage induction. Future work
334 using protocols designed specifically to observe these proteins could reveal further
335 instances of post-transcriptional regulation.

336 Our survey of protein upregulation during the *Caulobacter* DNA damage response led us
337 to identify post-transcriptional control of factors important for stress tolerance as
338 described above. Our work nominates putative Lon substrates that could contribute to
339 DNA damage tolerance and shows that DNA damage induced proteome changes are
340 dampened in ∆lon strains. Together, these data reveal that not all protein abundance
341 changes during the DNA damage response can be explained solely by canonical
342 transcriptional changes and highlights contributions from post-transcriptional regulation.

343 **METHODS**

344 **Bacterial strains and growth conditions**

345 Bacterial strains and plasmids used in this work are listed in Tables S9 and S10,
346 respectively. All *Caulobacter* strains used in this work are NA1000 derivatives.
347 *Caulobacter* strains were grown in PYE broth (2 g/L peptone, 1 g/L yeast extract, 1 mM
348 $MgSO_4$, and 0.5 mM $CaCl_2$). Solid media was made with 1.5% agar. Knockout strains
349 were created by replacing the native gene with a gentamycin resistance cassette using
350 the pNPTS138 non-replicating vector (38). Venus- and mKate2-expressing strains were
351 created by integrating pXGFPC-2 (39) based plasmids encoding fluorescent proteins
352 driven by a *lac* promoter (40) at the xylose locus.

353 **Bacterial growth curves**

354 An overnight culture was diluted into PYE at an OD600 = 0.05. A volume of 200uL of cells
355 was added to wells of a 96-well plate. Plate was shaken continuously at 30ºC and OD600
356 was read every 20 minutes in a BioTek Epoch 2 Microplate Spectrophotometer (Agilent,
357 Santa Clara, CA). MMC (0.5 µg/ml; Millipore Sigma, St. Louis, MO) was used to treat cells
358 with DNA damage.

359 **Western blot**

360 Western blots were performed using a commercially available rabbit anti-*E. coli* RecA
361 primary antibody (1:10,000 dilution; Abcam, Cambridge, MA, 16 hours). Blots were
362 visualized using the goat anti-rabbit Alexa Fluor™ Plus 800 secondary antibody (1:10,000
363 dilution; Licor, Lincoln, NE, 1 hour). Bands were quantified using ImageJ (41).

364 **Competition assays**

365 Overnight cultures of each test strain and the control strain were diluted to an OD600 =
366 1.0, mixed 1:1, and serially diluted 30,000-fold. Undiluted cells were analyzed with a
367 SpectraMax M2 microplate reader (Molecular Devices, San Jose, CA). Measurements
368 were taken for cell density (OD600), Venus fluorescence (Excitation 490nm, Cut off
369 515nm, Emission 530nm), and mKate2 fluorescence (Excitation 575nm, Cut off 590nm,
370 Emission 630nm). Diluted samples were grown to stationary phase (~48 hours, shaking
371 at 30°C) and optical density and fluorescence measurements were taken again. The
372 competitive index was calculated as the $\log_2$[((ratio test/control)END / (ratio
373 test/control))START / ((average ratio wild type test/control)END/[(ratio wild type
374 test/control))START].

375 **Sample collection and preparation for proteomics**

376 <u>Pre-damage sample</u>

377 Three biological replicates of overnight growth of each *Caulobacter* strain (wild type and
378 *Δlon)* were diluted to an OD600 = 0.0005 using PYE to a volume of 50mL and grown for
379 approximately 10 generations to an OD600 of 0.5-0.6. All samples were normalized to an
380 OD600 of 0.5 using PYE to a volume of 25mL. A 5 mL pre-damage sample was taken,
381 and cells were collected by centrifugation (6,000xg, 5min). Cell pellets were resuspended
382 in fresh lysis buffer (8M urea, 50mM HEPES pH7.5, 75mM NaCl), flash frozen, and stored
383 at -80˚C.

384 <u>Post-damage/pre-shutoff sample</u>

385 Cells were treated with 0.5 µg/mL MMC for 1 hour before cells were collected by
386 centrifugation (6,000xg, 10min) and resuspended in fresh PYE broth to an OD600 = 0.5
387 to a volume of 25mL. These treatment conditions are similar to those of the microarray
388 from the Laub lab (15) for simple comparison. Previous experiments indicate that the wild
389 type strain has about 55% survival to this treatment (38). After 2 hours, all samples were
390 normalized to an OD600 = 0.5 using PYE to a volume of 25mL. A 5 mL post-damage
391 sample was taken, and cells were collected by centrifugation (6,000xg, 5min). Cell pellets
392 were resuspended in fresh lysis buffer, flash frozen, and stored at -80˚C.

393 Post-shutoff sample

394 Cells were treated with chloramphenicol (30 µg/mL) for 2 hours. A 5 mL post-shutoff
395 sample was taken, and cells were collected by centrifugation (6,000xg, 5min). Cell pellets
396 were resuspended in fresh lysis buffer, flash frozen, and stored at -80˚C.

397 Sample preparation for proteomics

398 Samples were freeze-thawed three times in liquid nitrogen to aid cell lysis, then
399 centrifuged at 16,000xg for 10 mins at 4˚C. Supernatant was carefully transferred to a
400 fresh 1.5mL tube. A Bradford assay was performed to quantify protein concentration.
401 Because the Bradford assay is sensitive to high urea concentrations, a small fraction of
402 each sample was diluted 4-fold for the Bradford assay. 50 µg of each sample was
403 transferred to a fresh 1.5mL tube. The final volume was adjusted to 50µL using 100mM
404 Triethylammonium bicarbonate (TEAB) buffer.

405 To reduce disulfide bonds, 5 µL 200mM tris(2-carboxyethyl)phosphine (TCEP) was
406 added to each sample and incubated at 55˚C for 1 hour. To modify cysteine residues,
407 5uL of 375mM iodoacetamide was added to each sample and incubated 30 min at room
408 temperature in the dark. To precipitate protein, 6-volumes of cold acetone was added to
409 each sample, and they were stored overnight at -20˚C.

410 Samples were centrifuged at 8,000 x g for 10 min at 4˚C to collect precipitate. Supernatant
411 was carefully removed and discarded. Pellets were allowed to dry at room temperature
412 for 1 hour. Protein pelleted were resuspended in 100uL 50mM TEAB. Samples were
413 incubated overnight at 37˚C with 1.25 µg of trypsin (for a 2.5:100 ratio of trypsin to
414 protein).

415 **Tandem mass tagging for proteomics**

416 Samples were labelled using the TMT10plex™ Isobaric Label Reagent Set
417 (ThermoFisher Scientific, Waltham, MA, Catalog #90110) according to the product
418 instructions. Since each sample only contains 50 µg of peptides instead of the suggested
419 100 µg, half of each label was used per sample.

420 **Proteomics sample fractionation**

421 For each replicate experiment in each strain, equal volumes of each samples were
422 combined into a single tube and then dried in a SpeedVac. Pooled samples were
423 resuspended in 300 µL 0.1% TFA. Samples were dried in a SpeedVac a second time and
424 resuspended in 300 µL 0.1% TFA. The pH of each sample was measured to confirm that
425 it was between 2.5 - 3.5, which is critical for effective fractionation.

426 Pooled samples were fractionated using the Pierce™ High pH Reversed-Phase Peptide
427 Fractionation Kit (ThermoFisher Scientific, Waltham, MA, Catalog #84868) according to
428 the kit instructions. Fractions 1 and 5, 2 and 6, 3 and 7, as well as 4 and 8 were pooled
429 together for a final total of 4 fractions per sample. Samples were dried and resuspended
430 in 0.1% folic acid in water for mass spectrometry.

431 **Mass spectrometry for tandem mass tagging proteomics**

432 LC-MS analysis was performed, modified from (42) using an Easy-nLC 1000 nanoLC
433 chromatography system interfaced to an Orbitrap Fusion mass spectrometer
434 (ThermoFisher Scientific, Waltham, MA). Samples were pre-concentrated and desalted
435 on to a C18 trap column prior to separation over a 180-min gradient from 0% to 50%
436 mobile phase B (A:0.1% formic acid in water, B:0.1% formic acid in acetonitrile) at 300
437 nL/min flow rate with a 75 µm x 15 cm PepMap RLSC column (ThermoFisher Scientific,
438 Waltham, MA). Mass spectrometry parameters were as follows: ion spray voltage 2000V,
439 survey scan MS1 120k resolution with a 2 s cycle time, interleaved with data-dependent
440 ion trap MS/MS of highest intensity ions with charge state-dependent ion selection
441 window (z=2:1.2 m/z, z=3:0.7 m/z, z=4-6:0.5 m/z) and CID at 35% normalized collision
442 energy. Additionally, the top 5 (z=2) or 10 (z>2) product ions were synchronously selected
443 for HCD MS^3 at NCE 65% with Orbitrap detection to generate TMT tag intensities.

444 **Proteomics Data Analysis**

445 RAW data files were analyzed in Proteome Discoverer 2.4 (ThermoFisher Scientific,
446 Waltham, MA) using the SEQUEST search algorithm against *Caulobacter crescentus*
447 NA1000 (NCBI Reference Sequence: NC_011916.1) database downloaded from

448 uniprot.org. The search parameters used are as follows: 10 ppm precursor ion tolerance
449 and 0.4 Da fragment ion tolerance; up to two missed cleavages were allowed; dynamic
450 modifications of methionine oxidation and N-terminal acetylation. Peptide matches were
451 filtered to a protein false discovery rate of 5% using the Percolator algorithm. Peptides
452 were assembled into proteins using maximum parsimony and only unique and razor
453 peptides were retained for subsequent analysis. Protein quantitation based on TMT ion
454 abundance was performed using a co-isolation threshold of 75% and SPS match
455 threshold 65%. Each TMT channel was normalized to total peptide amount and then
456 abundance scaled to average 100% for all proteins.

457 Protein abundances were then normalized to the averages of the 0 hour samples (Table
458 S1). Protein ratios (Table S2) were calculated using edgeR (43).

459 **ACKNOWLEDGEMENTS**

460 This work was supported by NIH/NIGMS R35GM130320 to P. Chien. The mass
461 spectrometry in this paper was performed by Dr. Stephen Eyles at the University of
462 Massachusetts Amherst Mass Spectrometry Core Facility in Amherst, MA
463 (RRID:SCR_019063). The *ΔfzlC* strain was a generous gift from Erin Goley's lab at Johns
464 Hopkins University, Baltimore, MD.

465 **REFERENCES**

466 1. Little JW, Edmiston SH, Pacelli LZ, Mount DW. 1980. Cleavage of the *Escherichia*
467 *coli lexA* protein by the *recA* protease. Proc Natl Acad Sci U S A 77:3225–3229.

468 2. Horii T, Ogawa T, Nakatani T, Hase T, Matsubara H, Ogawa H. 1981. Regulation of
469 SOS functions: purification of *E. coli* LexA protein and determination of its specific
470 site cleaved by the RecA protein. Cell 27:515–522.

471 3. Courcelle J, Khodursky A, Peter B, Brown PO, Hanawalt PC. 2001. Comparative
472 gene expression profiles following UV exposure in wild-type and SOS-deficient
473 *Escherichia coli*. Genetics 158:41–64.

474 4. Khil PP, Camerini-Otero RD. 2002. Over 1000 genes are involved in the DNA
475 damage response of *Escherichia coli*. Mol Microbiol 44:89–105.

476 5. Vogel J, Argaman L, Wagner EGH, Altuvia S. 2004. The small RNA IstR inhibits
477 synthesis of an SOS-induced toxic peptide. Curr Biol 14:2271–2276.

478 6. Darfeuille F, Unoson C, Vogel J, Wagner EGH. 2007. An antisense RNA inhibits
479 translation by competing with standby ribosomes. Mol Cell 26:381–392.

480 7. Fröhlich KS, Förstner KU, Gitai Z. 2018. Post-transcriptional gene regulation by an
481 Hfq-independent small RNA in *Caulobacter crescentus*. Nucleic Acids Res
482 46:10969–10982.

483 8. Godoy VG, Jarosz DF, Simon SM, Abyzov A, Ilyin V, Walker GC. 2007. UmuD and
484 RecA Directly Modulate the Mutagenic Potential of the Y-family DNA Polymerase
485 DinB. Mol Cell 28:1058–1070.

486 9. Cafarelli TM, Rands TJ, Godoy VG. 2014. The DinB•RecA complex of *Escherichia*
487 *coli* mediates an efficient and high-fidelity response to ubiquitous alkylation lesions.
488 Environ Mol Mutagen 55:92–102.

489 10. Friedhoff P, Li P, Gotthardt J. 2016. Protein-protein interactions in DNA mismatch
490 repair. DNA Repair (Amst) 38:50–57.

491 11. Neher SB, Flynn JM, Sauer RT, Baker TA. 2003. Latent ClpX-recognition signals
492 ensure LexA destruction after DNA damage. Genes Dev 17:1084–1089.

493 12. Gonzalez M, Rasulova F, Maurizi MR, Woodgate R. 2000. Subunit-specific
494 degradation of the UmuD/D' heterodimer by the ClpXP protease: the role of trans
495 recognition in UmuD' stability. EMBO J 19:5251–5258.

496 13. Pruteanu M, Baker TA. 2009. Controlled degradation by ClpXP protease tunes
497 the levels of the excision repair protein UvrA to the extent of DNA damage. Mol
498 Microbiol 71:912–924.

499 14. da Rocha RP, Paquola AC de M, Marques M do V, Menck CFM, Galhardo RS.
500 2008. Characterization of the SOS regulon of *Caulobacter crescentus*. J Bacteriol
501 190:1209–1218.

502 15. Modell JW, Hopkins AC, Laub MT. 2011. A DNA damage checkpoint in
503 *Caulobacter crescentus* inhibits cell division through a direct interaction with FtsW.
504 Genes Dev 25:1328–1343.

505 16. Modell JW, Kambara TK, Perchuk BS, Laub MT. 2014. A DNA Damage-Induced,
506 SOS-Independent Checkpoint Regulates Cell Division in *Caulobacter crescentus*.
507 PLoS Biol 12:e1001977.

508 17. Gozzi K, Salinas R, Nguyen VD, Laub MT, Schumacher MA. 2022. ssDNA is an
509 allosteric regulator of the *C. crescentus* SOS-independent DNA damage response
510 transcription activator, DriD. Genes Dev 36:618–633.

511 18. Prahlad J, Yuan Y, Lin J, Chang C-W, Iwata-Reuyl D, Liu Y, de Crécy-Lagard V,
512 Wilson MA. 2020. The DUF328 family member YaaA is a DNA-binding protein with
513 a novel fold. Journal of Biological Chemistry 295:14236–14247.

514 19. Liu Y, Bauer SC, Imlay JA. 2011. The YaaA protein of the Escherichia coli OxyR
515 regulon lessens hydrogen peroxide toxicity by diminishing the amount of intracellular
516 unincorporated iron. J Bacteriol 193:2186–2196.

517 20. Price MN, Wetmore KM, Waters RJ, Callaghan M, Ray J, Liu H, Kuehl JV,
518 Melnyk RA, Lamson JS, Suh Y, Carlson HK, Esquivel Z, Sadeeshkumar H,
519 Chakraborty R, Zane GM, Rubin BE, Wall JD, Visel A, Bristow J, Blow MJ, Arkin AP,
520 Deutschbauer AM. 2018. Mutant phenotypes for thousands of bacterial genes of
521 unknown function. 7706. Nature 557:503–509.

522 21. Xing S, Zheng W, An F, Huang L, Yang X, Zeng S, Li N, Ouenzar K, Yu L, Luo L.
523 2022. Transcription Regulation of Cell Cycle Regulatory Genes Mediated by NtrX to
524 Affect *Sinorhizobium meliloti* Cell Division. Genes (Basel) 13:1066.

525 22. Stein BJ, Fiebig A, Crosson S. 2021. The ChvG-ChvI and NtrY-NtrX Two-
526 Component Systems Coordinately Regulate Growth of *Caulobacter crescentus*. J
527 Bacteriol 203:e0019921.

528 23. Meier EL, Razavi S, Inoue T, Goley ED. 2016. A novel membrane anchor for
529 FtsZ is linked to cell wall hydrolysis in *Caulobacter crescentus*. Mol Microbiol
530 101:265–280.

531 24. Mahmoud SA, Aldikacti B, Chien P. 2022. ATP hydrolysis tunes specificity of a
532 AAA+ protease. Cell Reports 40:111405.

533 25. Liu J, Zeinert R, Francis L, Chien P. 2019. Lon recognition of the replication
534 initiator DnaA requires a bipartite degron. Mol Microbiol 111:176–186.

535 26. Bissonnette SA, Rivera-Rivera I, Sauer RT, Baker TA. 2010. The IbpA and IbpB
536 small heat-shock proteins are substrates of the AAA+ Lon protease. Mol Microbiol
537 75:1539–1549.

538 27. Bhat NH, Vass RH, Stoddard PR, Shin DK, Chien P. 2013. Identification of ClpP
539 substrates in *Caulobacter crescentus* reveals a role for regulated proteolysis in
540 bacterial development. Molecular Microbiology 88:1083–1092.

541 28. Gaougaou G, Shankar S, Liot Q, Constant P, Déziel E, Lacroix M. 2020. Gamma
542 irradiation triggers a global stress response in *Escherichia coli* O157:H7 including
543 base and nucleotides excision repair pathways. Microbial Pathogenesis
544 149:104342.

545 29. Zeinert RD, Ogdahl JL, Liu J, Yang Q, Du Y, Barros BB, Freddolino PL, Haynes
546 CM, Chien P. 2022. A legacy role for DNA binding of Lon protects against genotoxic
547 stress. bioRxiv https://doi.org/10.1101/317677.

548 30. Beam CE, Saveson CJ, Lovett ST. 2002. Role for *radA/sms* in recombination
549 intermediate processing in *Escherichia coli*. J Bacteriol 184:6836–6844.

550 31. Topilina NI, Novikova O, Stanger M, Banavali NK, Belfort M. 2015. Post-
551 translational environmental switch of RadA activity by extein–intein interactions in
552 protein splicing. Nucleic Acids Res 43:6631–6648.

553 32. Zhou B, Schrader JM, Kalogeraki VS, Abeliuk E, Dinh CB, Pham JQ, Cui ZZ, Dill
554 DL, McAdams HH, Shapiro L. 2015. The global regulatory architecture of
555 transcription during the *Caulobacter* cell cycle. PLoS Genet 11:e1004831.

556 33. Zheng M, Wang X, Templeton LJ, Smulski DR, LaRossa RA, Storz G. 2001.
557 DNA microarray-mediated transcriptional profiling of the Escherichia coli response to
558 hydrogen peroxide. J Bacteriol 183:4562–4570.

559 34. Silva LG, Lorenzetti APR, Ribeiro RA, Alves IR, Leaden L, Galhardo RS, Koide
560 T, Marques MV. 2019. OxyR and the hydrogen peroxide stress response in
561 Caulobacter crescentus. Gene 700:70–84.

562 35. Beaufay F, Quarles E, Franz A, Katamanin O, Wholey W-Y, Jakob U. 2020.
563 Polyphosphate Functions In Vivo as an Iron Chelator and Fenton Reaction Inhibitor.
564 mBio 11:e01017-20.

565 36. Kirchner M, Schneider S. 2017. Gene expression control by *Bacillus anthracis*
566 purine riboswitches. RNA 23:762–769.

567 37. Rasouly A, Pani B, Nudler E. 2017. A Magic Spot in Genome Maintenance.
568 Trends Genet 33:58–67.

569 38. Tashjian TF, Chien P. 2023. Clamp Loader Processing Is Important during DNA
570 Replication Stress. J Bacteriol 205:e0043722.

571 39. Thanbichler M, Iniesta AA, Shapiro L. 2007. A comprehensive set of plasmids for
572 vanillate- and xylose-inducible gene expression in Caulobacter crescentus. Nucleic
573 Acids Res 35:e137.

574 40. Persat A, Stone HA, Gitai Z. 2014. The curved shape of Caulobacter crescentus
575 enhances surface colonization in flow. Nat Commun 5:3824.

576 41. Schneider CA, Rasband WS, Eliceiri KW. 2012. NIH Image to ImageJ: 25 years
577 of image analysis. Nat Methods 9:671–675.

578 42. McAlister GC, Nusinow DP, Jedrychowski MP, Wühr M, Huttlin EL, Erickson BK,
579 Rad R, Haas W, Gygi SP. 2014. MultiNotch MS3 enables accurate, sensitive, and
580 multiplexed detection of differential expression across cancer cell line proteomes.
581 Anal Chem 86:7150–7158.

582 43. Robinson MD, McCarthy DJ, Smyth GK. 2010. edgeR: a Bioconductor package
583 for differential expression analysis of digital gene expression data. Bioinformatics
584 26:139–140.

585

586

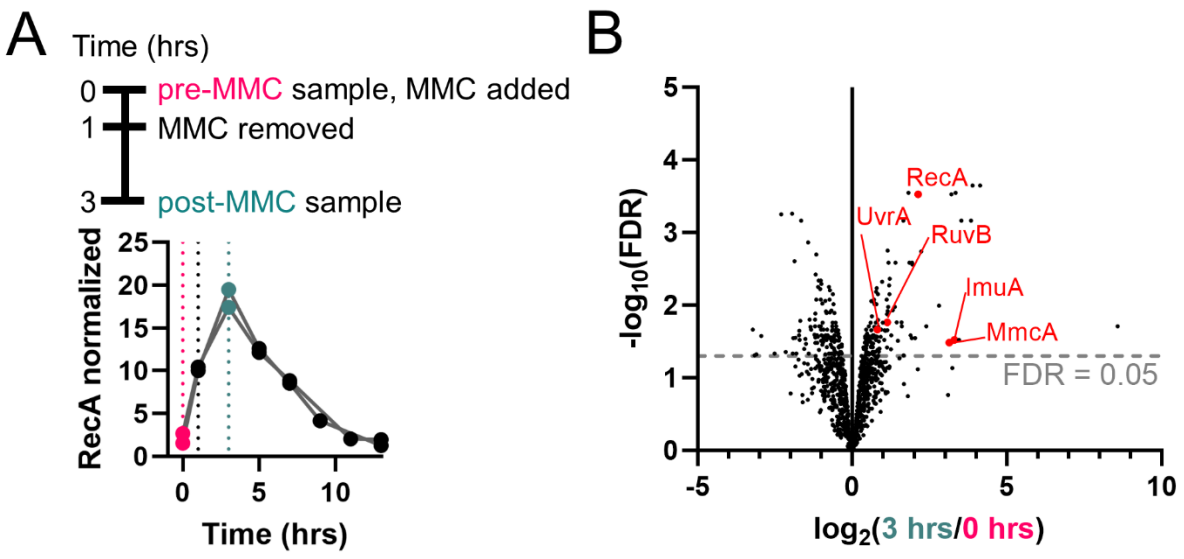

Figure 1. Proteomics reveals protein abundance changes during response to MMC treatment. (A) A western blot for RecA protein levels was used to determine when to sample for protein abundance changes after DNA damage treatment. Quantification of western blot for two replicates is shown, blot shown in Figure S1. Samples for proteomics were taken before treatment (0 hours, pink line). Cells were treated with MMC for 1 hour and recovered in fresh PYE for 2 additional hours before the post-treatment proteomics sample was taken (3 hours, teal line). RecA quantification was normalized to cross-reacting band for loading (Figure S1). (B) A volcano plot of proteomics data compares the statistical confidence (-$\log_{10}$(false discovery rate)) versus the $\log_2$(3 hrs/0 hrs). Several of the proteins that are significantly upregulated after DNA damage treatment are known DNA damage response proteins (highlighted in red). FDR indicates false discovery rate.

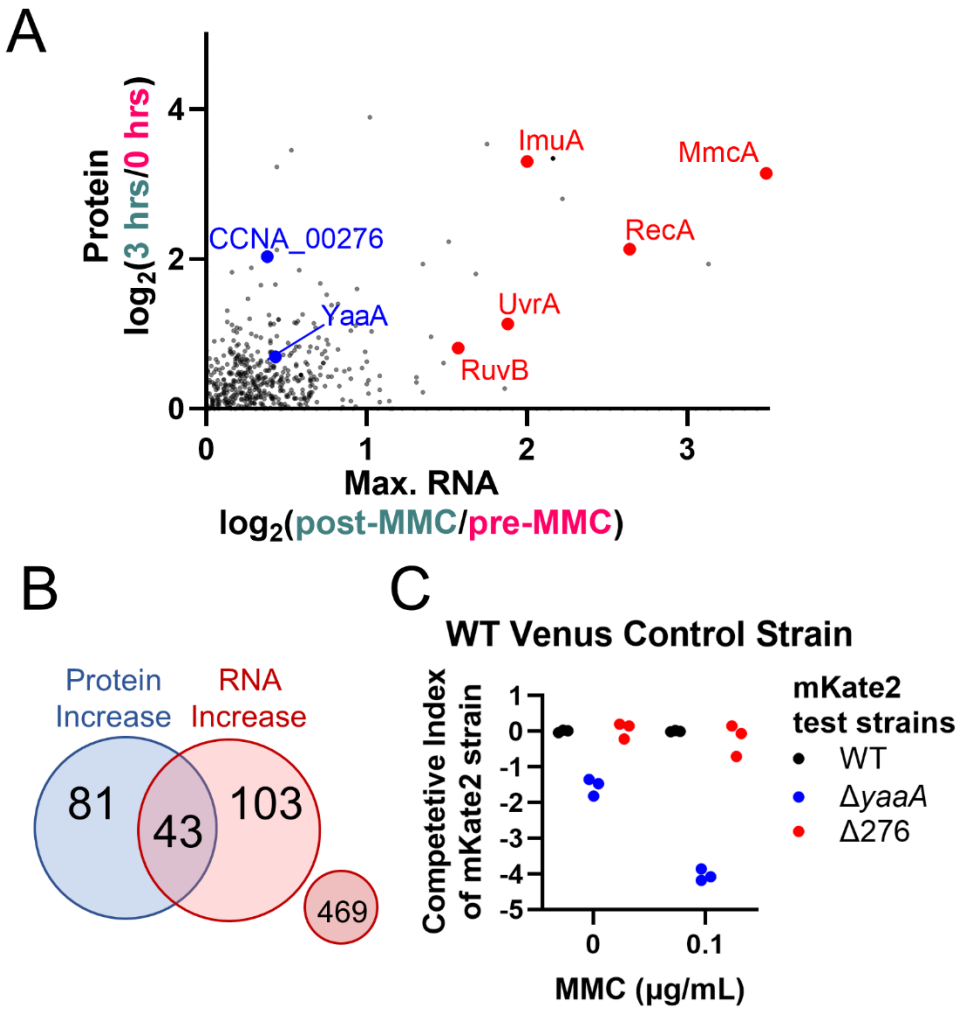

Figure 2. A comparison of proteomics and microarray data identifies proteins that are upregulated upon MMC treatment in a transcription-independent manner. A comparison between our proteomics and previously published microarray experiment that uses similar MMC treatment conditions (15) shows proteins that are upregulated upon DNA damage. Proteins highlighted in red are known DNA damage response genes that are upregulated at the RNA and protein levels. Proteins highlighted in blue are upregulated at the protein level, but not significantly upregulated at the RNA level and were identified by Tn-seq as potentially important for DNA damage survival. Graph

608 cropped to upper right quadrant to highlight proteins that are upregulated. One gene is
609 excluded (CCNA_03825) due to its extremely high induction to make other points more
610 visible. (B) A Venn diagram of proteins that are upregulated at the protein level (log_2(3
611 hrs/0 hrs) > 0, FDR > 0.05) and genes that are upregulated at the RNA level (log_2(post-
612 MMC/pre-MMC) > 1 standard deviation above the mean for all transcripts). The smaller
613 circle on the right side of this diagram reflects upregulated transcripts that were not
614 identified by proteomics. (C) When each mKate2-expressing test strain is competed in
615 co-culture against a wild type Venus-expressing fluorescent control strain, only the *ΔyaaA*
616 mutant shows a competitive disadvantage that is exacerbated by the presence of 0.1
617 µg/mL MMC. Reciprocal experiment in which test strains are marked with Venus and wild
618 type control is marked with mKate2 is shown in Figure S2D.

619

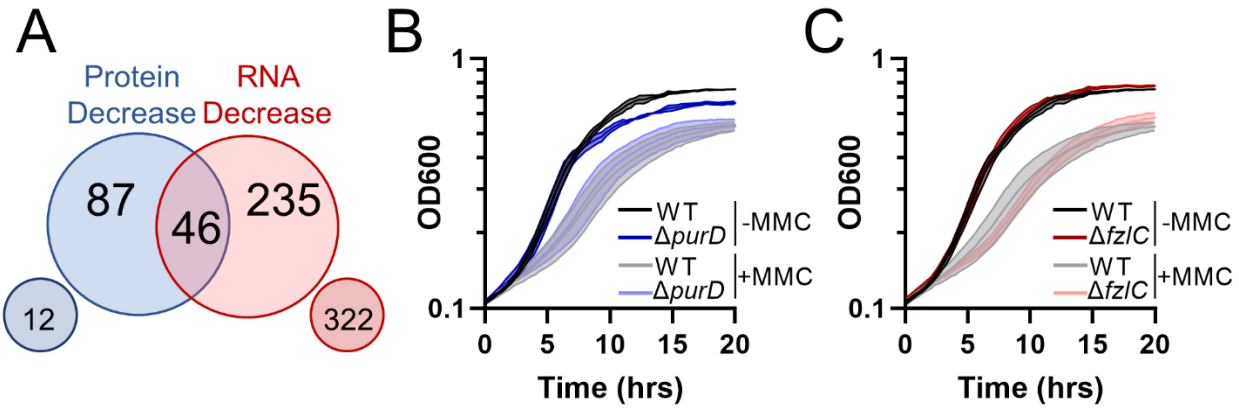

Figure 3. A comparison of proteomics and microarray data identifies proteins that are downregulated upon MMC treatment in a transcription-independent manner. The Venn diagram shows proteins that are downregulated at the protein level ($\log_2$(3 hrs/0 hrs) < 0, FDR < 0.05) and genes that are downregulated at the RNA level ($\log_2$(post-MMC/pre-MMC) > 1 standard deviation below the mean for all transcripts). The smaller circle on the left side of this diagram reflects proteins not identified in the microarray. The smaller circle on the right side reflects transcripts that were not identified in our proteomics. (B) The Δ*purD* strain has a stationary phase defect that is not observed in the presence of MMC. All experiments were performed in triplicate. Mean and standard deviation are shown. (C) The Δ*fzlC* strain show no difference in MMC sensitivity compared to the wild type strain. All experiments were performed in triplicate. Mean and standard deviation are shown. Same data for wild type controls are shown in (B) and (C) for ease of comparison.

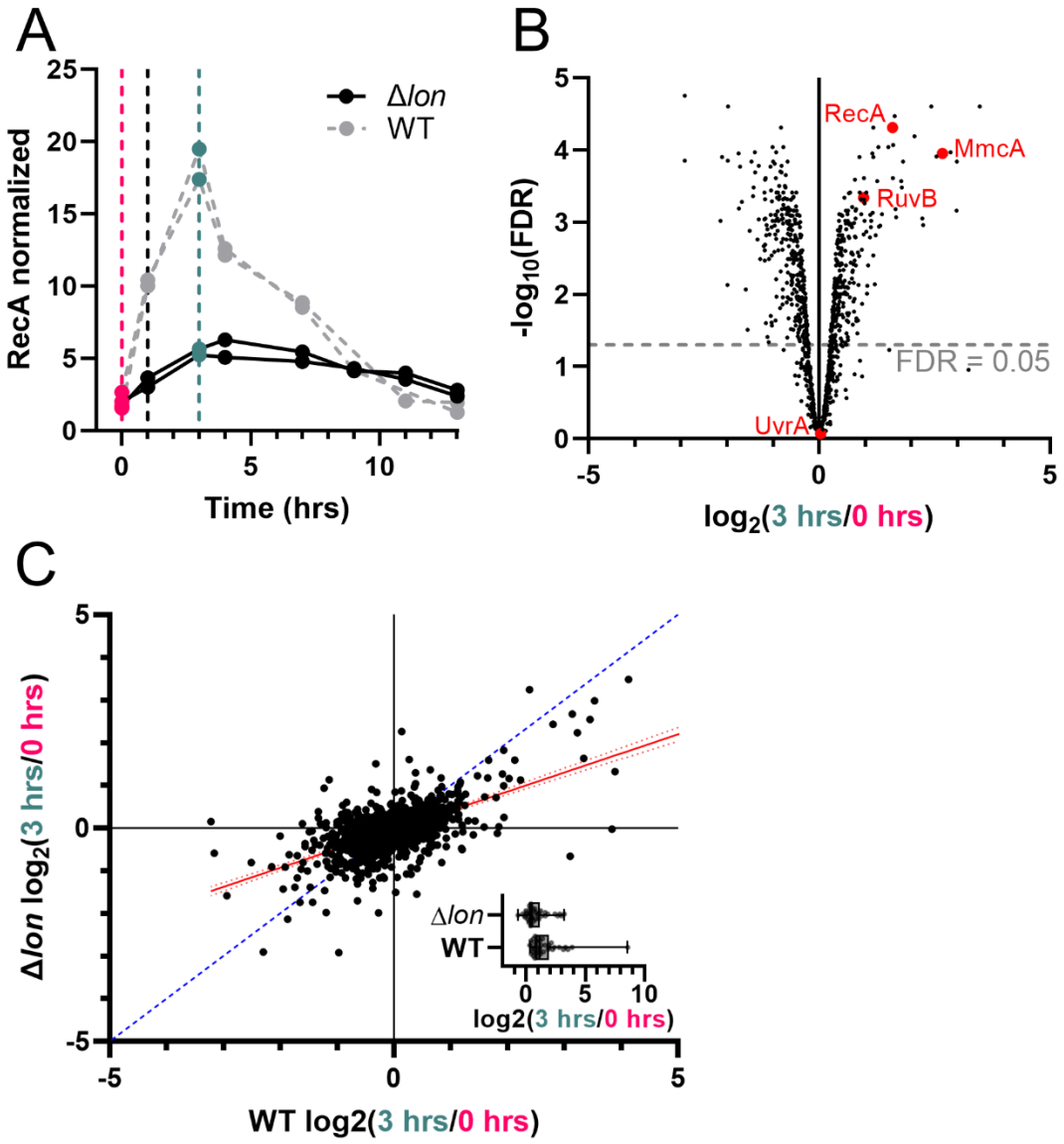

Figure 4. A similar set of DNA damage response proteins are upregulated in a Δ*lon* strain, but protein abundance changes are overall smaller. (A) A western blot to determine RecA protein levels was used to determine when to sample for protein abundance changes after DNA damage treatment in the wild type Δ*lon* strains. Note that the wild type data here is repeated from Figure 1A for easy comparison. Quantification of western blot for two replicates is shown, blot shown in Figure S1. Sampling for proteomics was performed as described in Figure 1A. RecA quantification was normalized to cross-

643 reacting band for loading (see Figure S1). (B) A volcano plot of proteomics data compares
644 the statistical confidence (-$\log_{10}$(false discovery rate)) versus the $\log_2$(3 hrs/0 hrs). Known
645 DNA damage proteins shown in Figure 1B are also highlighted here in red. ImuA was not
646 identified in the proteomics of the Δ*lon* strain and so is absent. FDR indicates false
647 discovery rate. (C) Comparison of the $\log_2$(3 hrs/0 hrs) for the Δ*lon* versus wild type strain
648 shows that fold changes of protein abundance are generally lower in the Δ*lon* strain. Blue
649 dashed line represents an y=x line. The red line represents the trendline of the data with
650 95% CI drawn (slope = 0.45). The inset plots $\log_2$(3 hrs/0 hrs) for all proteins that are
651 significantly upregulated (FDR <0.05).

652

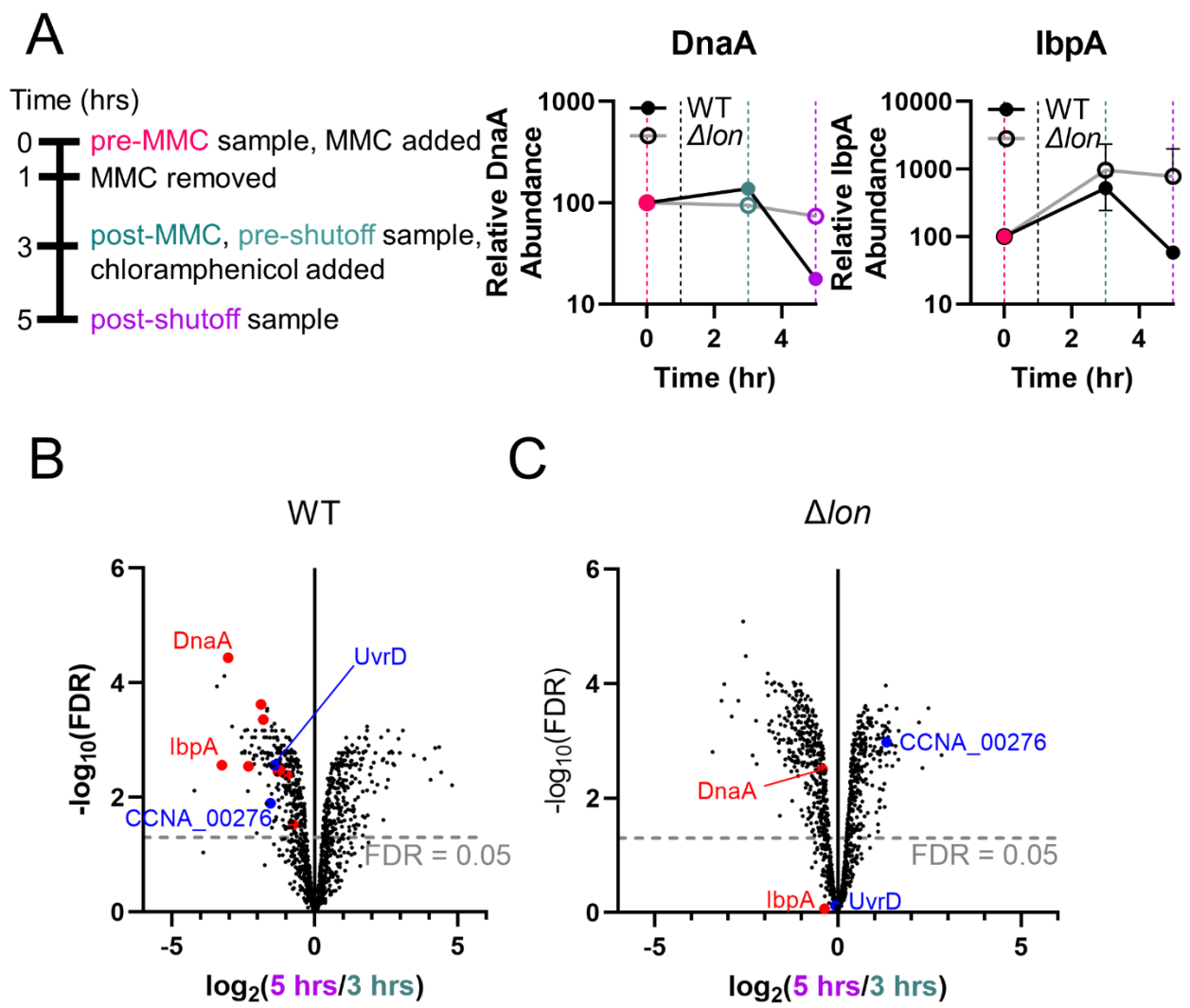

Figure 5. Proteomics revealed protein abundance changes when translation is shut off during the response to MMC treatment. (A) Proteomics results for changes in DnaA and IbpA protein abundance upon MMC treatment and subsequent translational shutoff. Samples for proteomics were taken before treatment (0 hours, pink line). Cells were treated with MMC for 1 hour and recovered in fresh PYE for 2 additional hours before the post-treatment proteomics sample was taken (3 hours, teal line). At 3 hours, cells were treated with chloramphenicol and final proteomics samples was taken after 2 additional hours (5 hours, purple line). Note that protein abundances are not directly comparable

662 between the two strains. Volcano plots compare the statistical confidence (-$\log_{10}$(false
663 discovery rate)) versus the $\log_2$(5 hrs/3 hrs) for (B) wild type and (C) Δ*lon* strains. Several
664 of the proteins that are significantly downregulated after chloramphenicol treatment are
665 known proteolysis substrates (examples highlighted in red in (A); see main text). Two
666 proteins of interest that will be discussed below are highlighted in blue. FDR indicates
667 false discovery rate.

668